Publ. Obs. Astron. Belgrade No. 49 (1995), 41-56

TOMOGRAPHIC IMAGING OF SOLAR-TYPE STARS

PRELIMINARY RESULTS FROM MUSICOS 1992 CAMPAIGN

S. JANKOV

Astronomical Observatory, Volgina 7, 11050 Belgrade, Yugoslavia

E-mail sjankov@aob.aob.bg.ac.yu

Abstract. In the past decade the methods of Tomographic Imaging proved to be a powerful tool to spatially resolve the surface and environment of stars. These techniques of indirect stellar imaging from photometry and spectroscopy allow to obtain, from the light curve and line profile disturbances (observed with high signal-to-noise ratio, spectral resolution and adequate phase coverage), an information about spatial distribution of quasistationnary structures in stellar atmospheres and environments. They have a wide range of application in stellar physics, particularly providing a knowledge of crucial importance to understand the stellar magnetic activity and physical processes related to it. We describe the scientific interest for tomographic interpretation of temporal photometric or spectroscopic variability along the rotational phase of solar-type stars. The basic principle of Tomographic Imaging of stellar surfaces is described, as well as the problem of regularization arising from the ill-posed nature of the inversion. We present the practical application based on data obtained from MUlti SIte COntinuous Spectroscopy (MUSICOS) international network of high resolution spectrometers around the world and we discuss the importance of such a program for systematic observations of long term spectroscopic and photometric variations of solar-type stars for the study of starspot distribution, active region evolution, differential motions and cyclic activity on time scales of several years and decades, in order to provide the stellar equivalent to the study of solar activity.

1. INTRODUCTION

1. 1. SOLAR-TYPE ACTIVITY ON STARS

The evidence collected from dedicated observations of several types of active stars in the past is strongly suggestive of a solar-type scenario with activity levels from the solar value to orders of magnitude higher. Activity phenomena are usually observed in red dwarfs, giants, T- Tauri and young stars, close late-type binaries because of deep convection zones and high rotation rates leading to differential rotation and efficient dynamos. They manifest themselves as flux variation in the continuum and emission lines over a wide range of wavelengths on timescales ranging from a few seconds, minutes (flares), hours and days (rotational modulation by active structures), to months and years (active region evolution, cyclic activity and differential motions).

The first evidence for stellar photospheric spots has been obtained from the photometric light curve periodic modulation. These quasi-sinusoidal flux variations are attributed (except an eventual eclipse) to the rotational modulation of a nonuniform distribution of photospheric spots. In the case of RS CVn and BY Dra systems the

slow migration (towards decreasing orbital phases) of these photometric waves has also been discovered (Catalano and Rodonò 1967), suggesting the change in the spot distribution over the surface. Systematic observations have shown almost sinusoidal light curves to become multipeaked or even flat, indicating also the variations in the spot number and size.

Some indirect indicators as the presence of TiO absorption bands in the spectra of fast rotating late-type stars in binary systems as HR 1099 implied that a substantial fraction of the photosphere must be spotted (Ramsey and Nations, 1980). By analogy with the Sun, the appearance of spots could be attributed to intense sub-photospheric magnetic fields which inhibit the convective energy transport until the surface. In particular the presence of dark spots and bright plages has been inferred from modeling the periodic low-amplitude photometric variations due to rotational modulation of spot-plage visibility (e.g. Rodonò et al 1986).

The rotational modulation of chromospheric emission in the Ca II H and K lines was shown for several RS CVn systems in the Mt Wilson H and K variability survey (Vaughan et al., 1981). Results from a joint IUE and ground based observations (Rodonò et al., 1987) have shown, for the RS CVn system II Peg, that the chromospheric and transition region emission reaches a maximum when the visible photometry is at minimum, thus indicating that chromospheric plages cover, in first approximation, an area correlated to the photospheric spots. Spot and plage modeling indicated that their physical characteristics are close to the solar ones, but they can cover up to 50% of the stellar surface (Byrne et al., 1987). Some empirical relations were established (Mangeney and Praderie 1984, Noyes et al. 1984) between the coronal or chromospheric activity and the rotational velocity through the Rossby number, suggesting that the heating is related to the production of magnetic energy through a dynamo mechanism. Also the rapid variations in X-ray, radio and in the optical occurring on dMe, RS CVn, T-Tauri, etc. stars are reminiscent of flares as observed on the Sun.

However, little was known about the actual distribution of those magnetic structures and activity phenomena before the advent of high signal-to-noise observations with CCD and Reticon detectors has stimulated the development of quantitative mathematical methods for studying the spatially resolved stellar surfaces by the means of Doppler Imaging methods. These methods allow, for the first time, to compare the photospheric images with the signatures of chromospheric, transition region or coronal emission, to describe the vertical stratification and energy balance of magnetic structures and to monitor the changes, associated with active region behaviour, over months and years in order to track differential motions, and constrain theories of internal rotation and dynamo.

1. 2. DEVELOPMENT OF DOPPLER IMAGING TECHNIQUE

The intensity rotational modulation gives a one dimensional projection in longitude of the surface structures. It provides an indirect way of *imaging* the star i.e. recovering the information not only in longitude L but also in latitude B. In a method developed by Deutsch (1970) for chemically peculiar stars, the variation of line equivalent widths has been adjusted by parameters describing the development in spherical harmonics

of the stellar surface inhomogeneities. This method did not make full use of the profile, mainly due to the low spectral resolution and low signal-to-noise ratio available then on photographic plate spectra.

Khokhlova and Ryabchikova (1970, 1975) and Falk and Wehlau (1974) proposed to use the full information contained in the line profile. Khokhlova and Ryabchikova modelised the local abundances for two Ap stars using a trial-and-error profile fitting.

Different formulations of the Doppler Imaging method have been proposed or applied to various observations. Goncharskij et al. (1982) formulated the problem of finding local abundances, for Ap stars, in terms of an integral equation assuming that the emission intensity in the continuous spectrum does not depend on the position. Vogt and Penrod (1983) gave the physical principle of Doppler Imaging of late-type stars and used a trial-and-error profile fitting method to reconstruct the stellar map.

A simple variant of the Doppler Imaging method has been applied by Gondoin (1986), to observations of HR1099, by identifying bumps components in the profile and following their velocity changes with rotational phase. Neff (1988), Walter (1987) and collaborators have developed a spectral imaging method adjusting IUE Mg II emission spectra of the system AR Lac with a minimal number of components.

Vogt et al. (1987) described the method of Doppler Imaging for spotted solar-type stars expressing the relation between local surface intensities and the observed spectral profile in matrix form by approximating the projection matrix as the marginal response of data pixel to changes in image pixel. To obtain the image-data transformation they assumed that the spot does not make a significant contribution to the observed flux, and the shape and strength of the line profile is the same in the spot as it is in the photosphere.

Jankov (1987) developed the methods of tomographic indirect stellar imaging from projections, based on the principle of flux rotational modulation, giving a full mathematic formulation in terms of matricial formalism, in the general case in which both spot and photosphere make a significant contribution to the observed line, treating explicitly the problem of nonlinearity of the image data transformation due to variable continuum flux level of spotted solar-type stars. In the Tomographic Imaging approach the problem of image reconstruction from spectroscopy and the problem of image reconstruction from photometry has been treated with the same mathematical formalism.

2. PRINCIPLE AND METHOD OF STELLAR TOMOGRAPHIC IMAGING

Comparing with imaging from photometry the Doppler Imaging approach provides an additional axis spatially resolved and the possibility to map different levels of the stellar 3-Dimensional atmosphere by using selected spectral lines. In addition, the available signal-to-noise from ground based photometry is not sufficient to obtain the required image resolution.

However the constraints from photometry dimension are important since they allow to obtain the better reliability of the reconstructed image (Jankov and Foing 1992). Moreover the high-speed and high signal-to-noise photometry from space can provide

the sufficient resolution in order to constraint the Tomographic Imaging of velocity fields (Jankov, in preparation).

Here we describe the principle and method for flux rotational modulation imaging of solar-type stars, treating the problem of indirect stellar imaging from projections to recover the *specific intensities* on the surface of a star, from its integrals (fluxes) over the parts of the stellar surface observed at different angles of view.

The approach concerns only the determination of the specific intensities on a stellar surface, supposing the local velocity and magnetic fields to be *a priori* known or negligible. In fact, when dealing with imaging of photospheres, in the optical wavelength regions, the variation of contribution due to inhomogeneous velocity fields and moderate magnetic fields (Zeeman splitting) can be assumed to be negligible comparing with the rotational broadening of fast rotators.

Since one cannot observe directly the specific intensities, but only their integrals over the apparent stellar disc, i.e. the fluxes, the projection r is defined as the flux-type integral :

$$P_r = \iint_{\Gamma_r} I_c(M, \lambda_0)[1 - \varepsilon + \varepsilon \cos \Theta_{rk}] \cos \Theta_{rk} \mathrm{d}S \tag{1}$$

where $I_c(M, \lambda_0)$ is the intensity distribution on a star, $\cos \Theta_{rk}$ is the angle between the line of sight and the outward normal of the k-th element of the stellar surface $\mathrm{d}S$, ε is limb darkening coefficient, and Γ_r represents the domain of integration for the flux detected in the corresponding detector pixel of the spectrograph or for the flux detected by the photometer. The domain Γ_r is determined by the projection onto a stellar surface (Fig. 1) of a) the constant velocity strip for the case spectroscopic data b) the visible stellar disc for the case of photometric data.

The principle of Doppler Imaging is shown on Fig. 1. When a signal from the spot is detected at some velocity, the spot position will be undetermined in the domain of the projection of the corresponding constant velocity strip (dark shadowed region). During the stellar rotation the same spot will be detected in some other velocity position, whose projection domain is depicted with the light shadowed region. The spot position can be determined as an intersection of two shadowed regions.

However, the stellar surface is mapped using the complete set of domains for all detector pixels obtained for different angles of view as shown in Fig. 2 for the case of Doppler Imaging and in Fig. 3 for the case of imaging from photometry. Note that for the case of imaging from photometry the details above the subobservers latitude can be localized only by the supplementary flux modulation due to the different surface projection when the detail is turning around the pole.

Given a number of projections at different angles of view, the estimation of the corresponding distribution $I_c(M, \lambda_0)$ on the stellar surface is the basic problem of the image reconstruction from available types of observations.

In practice the strict surface integrals (1) have to be replaced by the strip integrals because of the unavoidable limits set by the resolution of the instrument. So, the image resolution should be finite and one can use $N_L \times N_B$ digitization in which the picture region is divided into $J = N_L \times N_B$ array of pixels that will be referred to as the resolution pixels.

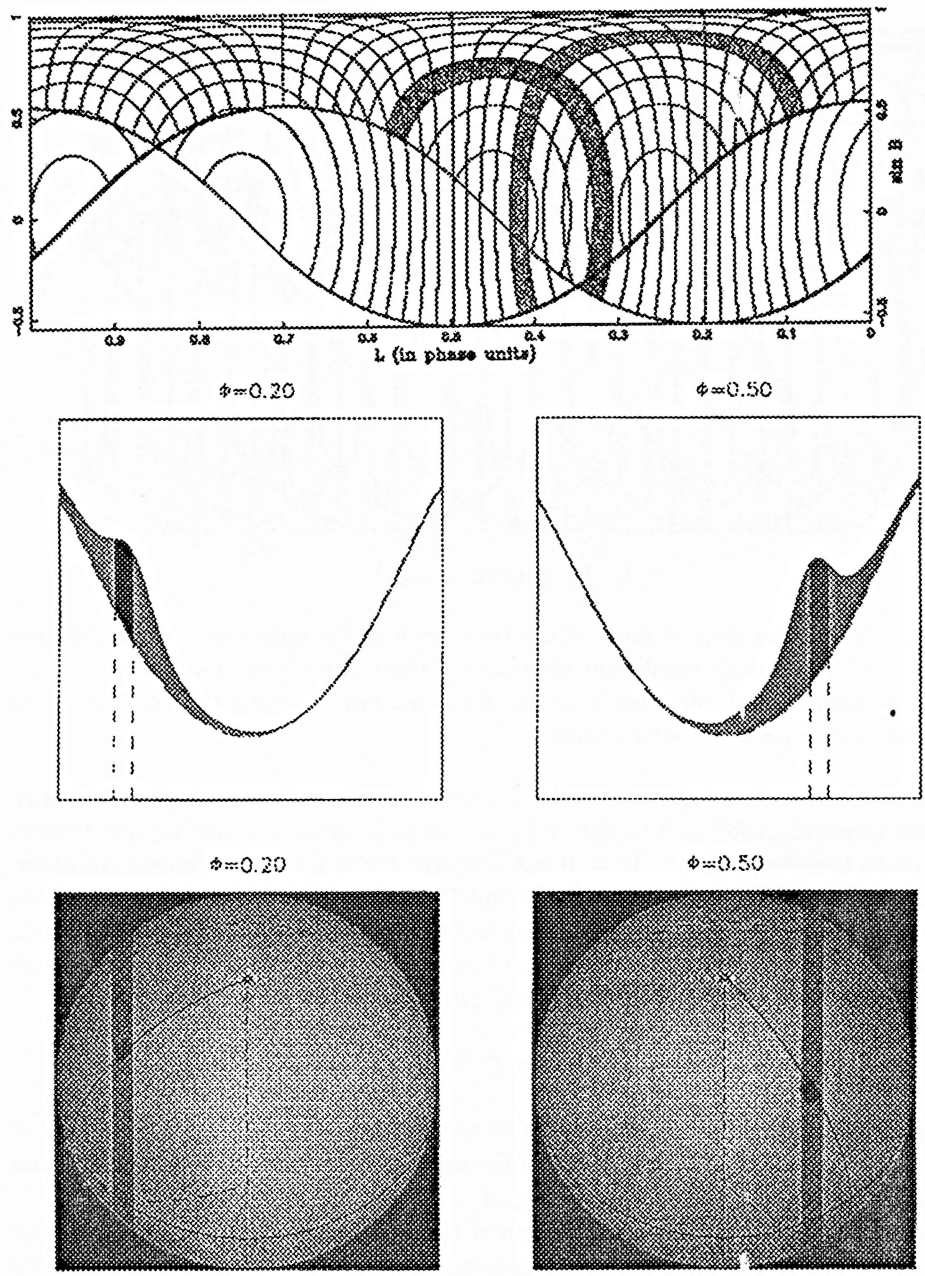

Fig. 1. The principle of localization of stellar surface details by intersection of two domains Γ_r corresponding to the two different angles of view (phases). The shadowed regions depict the projection of the constant velocity strips onto a stellar surface. The parts of the stellar surface visible at the particular phases are limited by the stellar limb here projected as the lower envelopes of equal velocity strips.

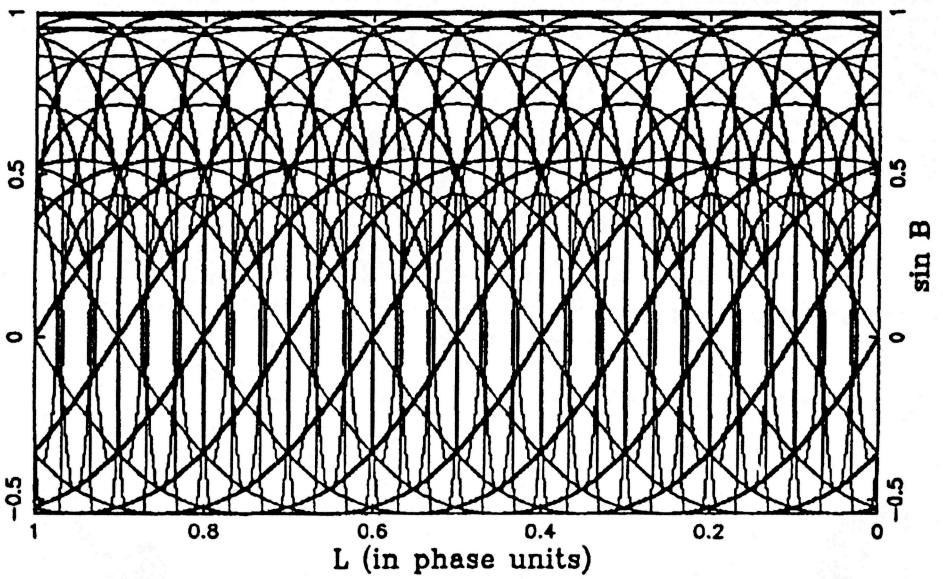

Fig. 2. Doppler Imaging network. The network on a stellar surface as it is formed when the star is observed in 10 equidistant view angles (phases), while the projected rotational velocity is resolved by the detector in 10 resolution elements. Basically this network is used to localize the details on a stellar surface.

Algorithmically that leads to the discretization of the problem and allows to translate the physical problem into the indirect imaging terms considering the general image-data transformation : $Y_{\mathrm{I}} = \mathbf{R} * X_{\mathrm{J}}$, where J and I are the dimensions of the image space and data space respectively and **R** is a mapping which takes a function in the image (X_j) space into a function in the data (Y_i) space. In our case the image X_{J} concerns the distribution of stellar surface brightness $I_c(M, \lambda_0)$ and the operator **R** is described by some combination of the integrals (1) :

$$\mathbf{R} = f(P_r).$$

In the case of Photometry Imaging the image is mapped into a light curve and in the case of Doppler Imaging the effect of the operator **R** is described by the dynamic difference spectrum, as illustrated on Fig. 4.

Jankov (1987) showed that the problem of Doppler Imaging can be fully linearized when the *shape* of the local spectrum does not depend on the position on a stellar surface while the problem of imaging from photometry is intrisically linear. In practice, to benefit for the linearized image-data transformation, one should choose the spectral line with low sensitivity to the temperature. Note also, that in solar-type scenario, for the stellar photospheres (where the brigt plages are several hundred Kelvins hotter and dark spots are several thousand Kelvins cooler than surrounding), the effect of the line profile dependence is cancelled since the surface brightness is proportional to

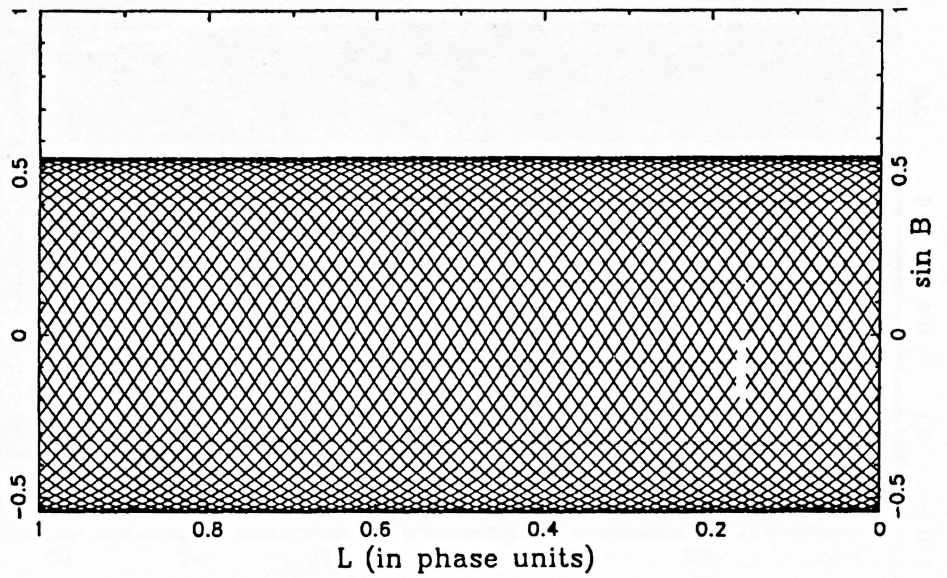

Fig. 3. Photometry Imaging network. The network on a stellar surface as it is formed when the star is observed in 50 equidistant view angles (phases). This network is formed only by the stellar limb and provides the enhanced photometrical rotational modulation. Basically this network is used to localize the details on a stellar surface below the subobservers latitude.

$T_{\rm eff}^4$, and the coolest spot regions do not contribute significantly to the observed line. For this reason the dependence of the local line profile on temperature is important only in the limited range of several 100 Kelvins around the photospheric temperature.

In such a way the operator **R** can be replaced by a matrix $R_{\rm IJ}$ and the problem can be formulated in the linear representation :

$$Y_i = \sum_{j=1}^{\rm J} R_{ij} X_j \qquad i = \overline{1,\rm I}. \tag{2}$$

In the general case, when the shape of the local line profile depends on the position on a stellar surface as a function of limb angle and local physical conditions (temperature, pressure, etc.), the image-data transformation can be still represented by the equation (2), (Jankov, 1992), however it is intrisically non-linear since the entries of the projection matrix $R_{\rm IJ}$ depend on the image vector $X_{\rm J}$. In that case, the entries of the matrix $R_{\rm IJ}$ cannot be evaluated analytically, but using line synthesis programs with an accurate model of stellar atmosphere (including full temperature and limb angle dependence of the line profile).

However, neglecting the limb angle dependence of the *shape* of the local line profile the grid of the spectra of the homogeneous, non-rotating standard stars with surface temperatures in the range from spot to surface temperature of the star under investigation, can be used to obtain the corresponding entries of the matrix $R_{\rm IJ}$ and

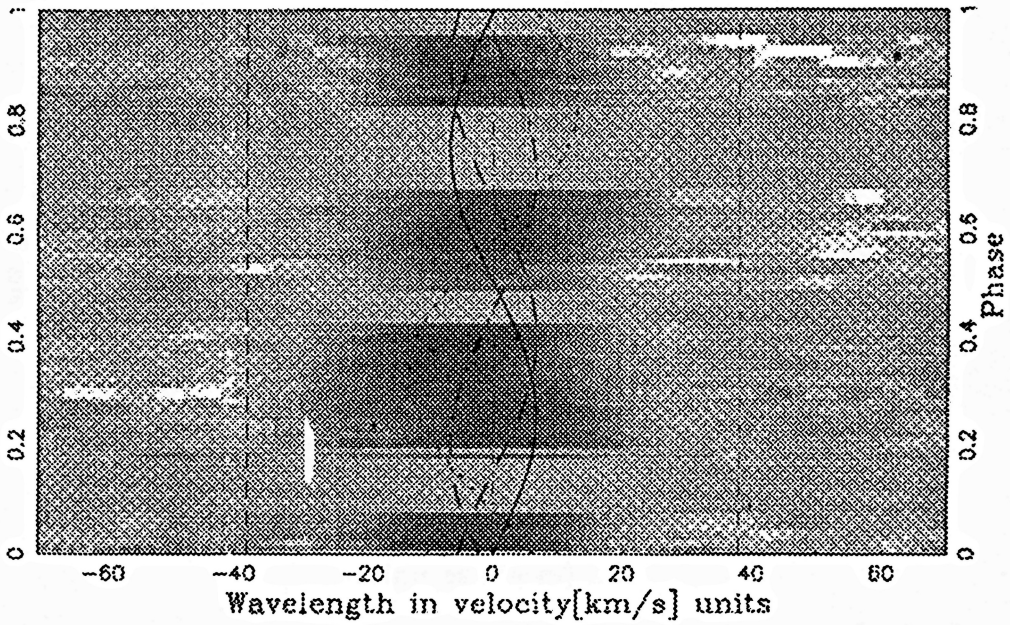

Fig. 4. Dynamic difference spectrum. This spectrum is arranged from sixty difference spectra where immaculate star line profiles are substracted from spotted star line profiles observed during the campaign. The projected velocity curves of the spots which positions are determined posterior to reconstruction are also presented. The stellar surface is extended over the rotational profile limits, depicted as vertical dashed lines, due to the convolution with the intrinsic line profile.

to complete the formulation of the problem. Since the limb-angle dependence of the local line profile has smaller influence on the integrated line profile than possible weak blends, a grid of observed spectra used as model input of the imaging code is likely to yield more accurate results than a table of synthetic profiles because the undetected blends are automatically excluded.

Again, considering only the spot regions that make a significant contribution to the observed line, one can use a grid of spectra of reference stars in the limited range around the photospheric temperature of the star to be imaged in order to handle the Tomographic Imaging reconstruction with the required degree of accuracy.

3. INVERSE PROBLEM

3. 1. SOURCES OF THE ILL-POSED NATURE OF THE INVERSE PROBLEM

The task of the indirect imaging reconstruction problem is to recover the image function X_J from the observed set of data Y_I. Generally, that task is not a trivial one because the matrix R_{IJ} can be singular and the solution X_J does not exist as R_{IJ}^{-1}

does not exist. Even if R_{IJ}^{-1} exists, there can be more than one R_{IJ}^{-1}, the nature of which is used being dependent on X_J and in that case the solution is not unique (Jankov and Foing, 1992). In the presence of noise, the question of existence, uniqueness, stability and image resolution are, generally, closely related, except if one deals with the star with the inclination not close to $\pi/2$ or to 0 where only the problem of stability remains.

In the noiseless and infinitely resolved world, Eq. (2) should be considered, (since there should not be a star, which inclination equals exactly 0 or $\pi/2$), as a solution does exist and is unique if $rank(R_{IJ}) = I = J$.

However, in the real world the question of fundamental practical importance is whether the solution is stable against small perturbations in the data function. In our case the matrix R_{IJ} is badly conditioned and the problem of the image reconstruction is fundamentally ill-posed, thus high performance regularization algorithms are crucially needed.

In addition to the noise in the observed profiles there are three principal sources of the ill-posed nature of the problem of inversion of the equation (2) in the Doppler Imaging approach :

a) Incompleteness of data

b) The projection matrix R_{IJ} is determined by the estimated quantities (the parameters determining the orientation of the star and orbital elements of a binary system) containing systematic and random errors.

c) Some details of the stellar surface are observed in non-optimal conditions (close to limb). Using the complete set of spectra for all observed phases, the image is spanned by the related strips, producing the global instability.

3. 2. MAXIMUM ENTROPY REGULARIZATION

The regularized solution can be obtained by minimizing an appropriate "regularizing functional", of the image function subject to the classical constraint $\chi^2 = \chi_0^2$:

$$\sum_{i=1}^{I} \left((Y_i - \sum_{j=1}^{J} R_{ij} \hat{X}_j)/\sigma_i \right)^2 = \chi_0^2$$

where χ_0^2 is determined by the required confidence level to data statistics χ^2, $\hat{X}_J$ is the solution, and σ_i is the standard error on datum i. The data statistic χ^2 is used to measure the discrepancy between observed and modeled data, while the χ^2 surfaces are convex ellipsoids in J dimensional image space.

To deal with the problem of the ill-posed nature of the inversion, the supplementary information should also be used in the form of well suited additional observations, as for example the temperature constrains from VRI photometry, or *a priori* information imposed on spectra or on the stellar image.

There are various alternatives for the choice of the regularizing functional each of them defining different methods of regularisation (Titterington, 1985). The choice of the regularizing functional depends generally on the prior information about the image function. Choosing the Kullback-Leibler distance one deals with the maximum

entropy approach where the solutions are chosen by maximizing the configurational entropy with respect to the the prior solution ${}^0X_J$:

$$\sum_{j=1}^{J} \hat{X}_j ln(\hat{X}_j / {}^0X_j).$$

Since the χ^2 surfaces are convex ellipsoids in image space and entropy surfaces are also strictly convex there is an unique point on the hypersurface $\chi^2 = \chi_0^2$ possessing the greatest entropy and the maximum entropy reconstruction is unique for the given data sample (Skilling and Bryan 1984).

4. RESULTS FROM MULTI-SITE OBSERVATIONS

4. 1. OPTIMAL STRATEGY OF OBSERVATIONS

In order to obtain the Doppler Image with the required number of resolved elements on the stellar surface, the strategy of observations, consistent with the spectral and temporal resolution, should be defined. Since one can have access only to strip integrals, when it is a question of spectroscopic data, we are in fact limited in the amount of information we can extract about the original distribution. The consequence is that, in practice, a finite number of phases to be observed suffice, and once this sufficient set of phases have been observed, the additional observations will contribute no more information than repetition of existing phases would contribute. If the star is resolved in latitude by N_L equivalent zones, N_L being proportional to the product of rotational velocity of the star and spectral resolving power, the complete set of data is obtained by observing each of the resolved zones in the central meridian i.e. by observing the star in $N_\Phi = N_L$ equidistant phases.

The other important parameter is the finite exposure time of the spectrum and corresponding spectrum signal-to-noise ratio. For the fixed duration of the observations, the image resolution limit is determined by the spectral and temporal resolution. Spectral and temporal resolution are determined by the noise thus, finally, the image resolution, and also the quality of the restoration, for optimally sampled data, are limited by the signal-to-noise ratio. We note that, in principle, the regularization algorithms using the *a priori* information allow some degree of super resolution by providing an the solution even in the case when $J > I$. However, in the case of indirect stellar imaging, one should not pretend to get much more resolution than allowed by the data.

The strategy of observations is also determined by other scientific goals that require :

a) a continuous observation ideally covering at least 2 rotational periods of the system in order to distinguish transient phenomena (as stellar flares) from the rotational modulation. In particular, for the stars with periods close to one day, a convenient phase coverage is impossible to obtain without continuous observations,

b) repeated observations of the same object in order to follow the evolution of the active structures.

On the basis of previous discussion, one can see that the optimal strategy of observations linked to Tomographic Imaging requires continuous spectroscopic monitoring over the rotational period of the star. To achieve the listed requirements a specific observational program was designed. MUSICOS (MUlti-SIte COntinuous Spectroscopy) is an international program (Catala et al. 1993) whose task is to facilitate continuous spectroscopic coverage of stars, using multi-site observations on existing telescopes of the 2m class distributed around the world. The observational campaigns are organized as frequent as possible in order to monitor the long term activity of selected targets.

4. 2. OBSERVATIONS AND IMAGE RECONSTRUCTION OF HR 1099

The second MUSICOS campaign was organized in December 1992 using the spectrographs existing on-site and fiber-fed MUSICOS spectrograph that was transported to Mauna Kea (Hawaii). Sixty high-resolution and high signal-to-noise ratio CCD spectra of the RS CVn binary system HR 1099 (K1 IV+G5 V) were obtained during the campaign at Observatoire de Haute-Provence, France (OHP) Beijing Astronomical Observatory, China (BAO) and University of Hawaii, USA (UH).

At OHP the AURELIE spectrograph, equipped with a Thomson 2048 pxl linear detector, yielding a wide spectral range ($\approx$ 6370–6490 Å) at a spectral resolution of 30 000, was used. The data reduction was carried out with the help of the MIDAS image processing system running on a Vax 4500 computer at Meudon Observatory.

At BAO, the ISIS fibre-spectrograph coupled with a 6-slice Bowen-Walraven image slicer allowed maximal throughput at a spectral resolution of 31 000. With a Tektronix 512×512 pxl detector, the spectra span 36 Å around 6434 Å. The data were reduced using the optimal extraction procedure of Horne (1986).

At UH, the MUSICOS spectrograph (Baudrand & Böhm 1992) was used. With a Tektronix 2048×2048 pxl detector, 64 orders are obtained in a single exposure, covering a spectral domain ranging from 4370 to 8760 Å at a spectral resolution of 30 000. The data were reduced using a dedicated software called MUSBIC. In this preliminary analysis though, we use order #88 only, which contains the classical Ca I and Fe I Doppler Imaging lines spanning about 100 Å around 6420 Å.

The details of the data acquisition and reduction are given in Jankov and Donati (1994).

The technique was applied to the moderately strong photospheric absorption Ca I λ 6439 Å line in order to recover the image of the photospheric surface of the primary star. The image reconstruction was performed using the spectra of the standard star HR 3762 (K0) for the primary component of HR 1099, and HR 4182 (G5) for the companion. The fundamental stellar parameters (listed in Table I) and orbital elements were adopted from Fekel (1983).

The spectra of standard stars were broadened by the rotational profile calculated using the values listed in Table I and shifted to the wavelength corresponding to the orbital motion. Contribution of each spectrum was determined using the values of effective temperature, radius, limb darkening coefficient and the photometric light curve. Fig 5 shows the photometry of HR 1099 obtained during the campaign (around the Julian date 2449000) but also four years before and one year after.

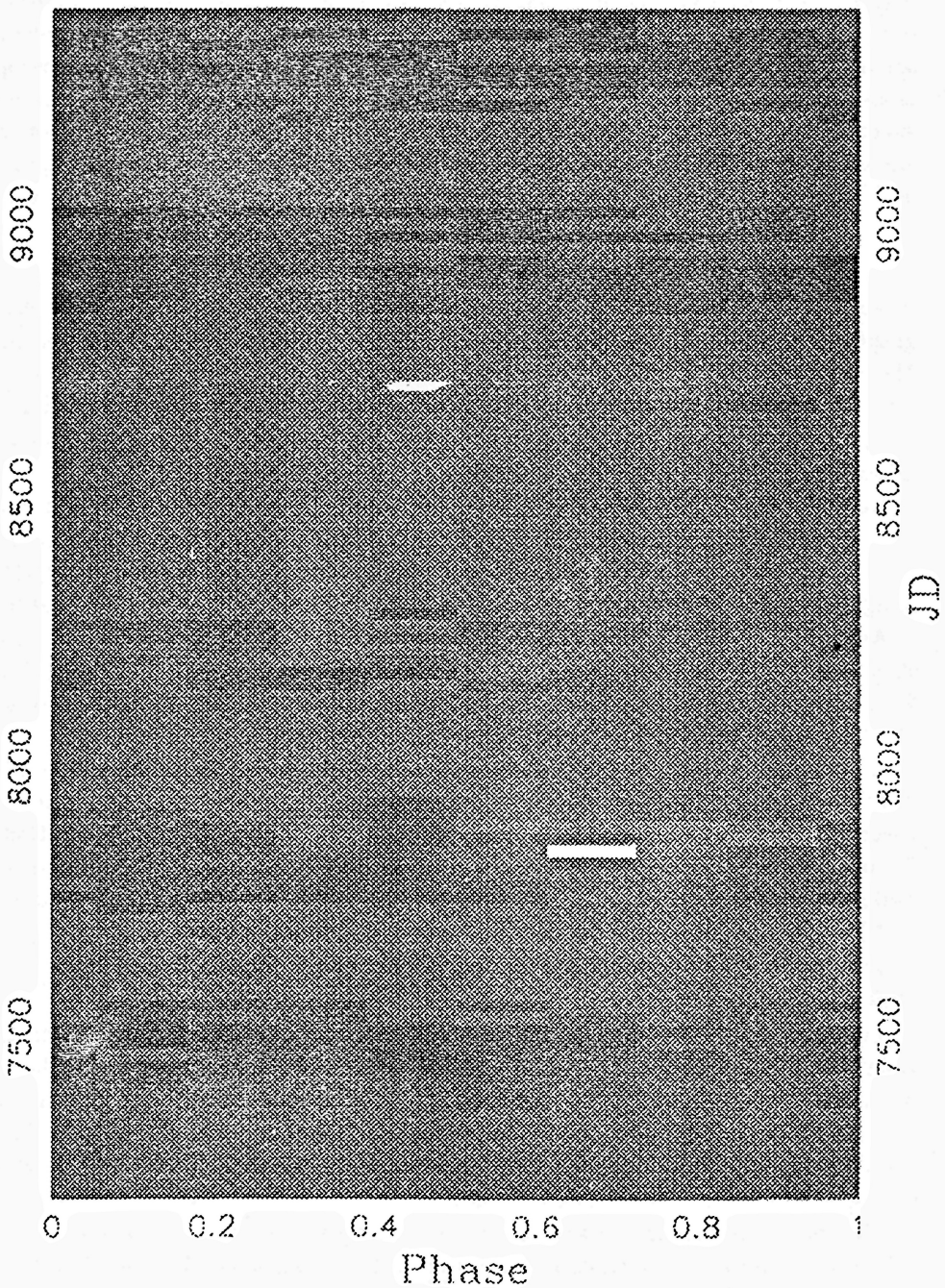

Fig. 5. APT photometry of HR 1099 from 1988 to 1993. The maximum and minimum fluxes detected in that interval are white and black respectively, intermediate values are represented by corresponding levels of gray while the uniform gray areas represent the intervals with available photometry.

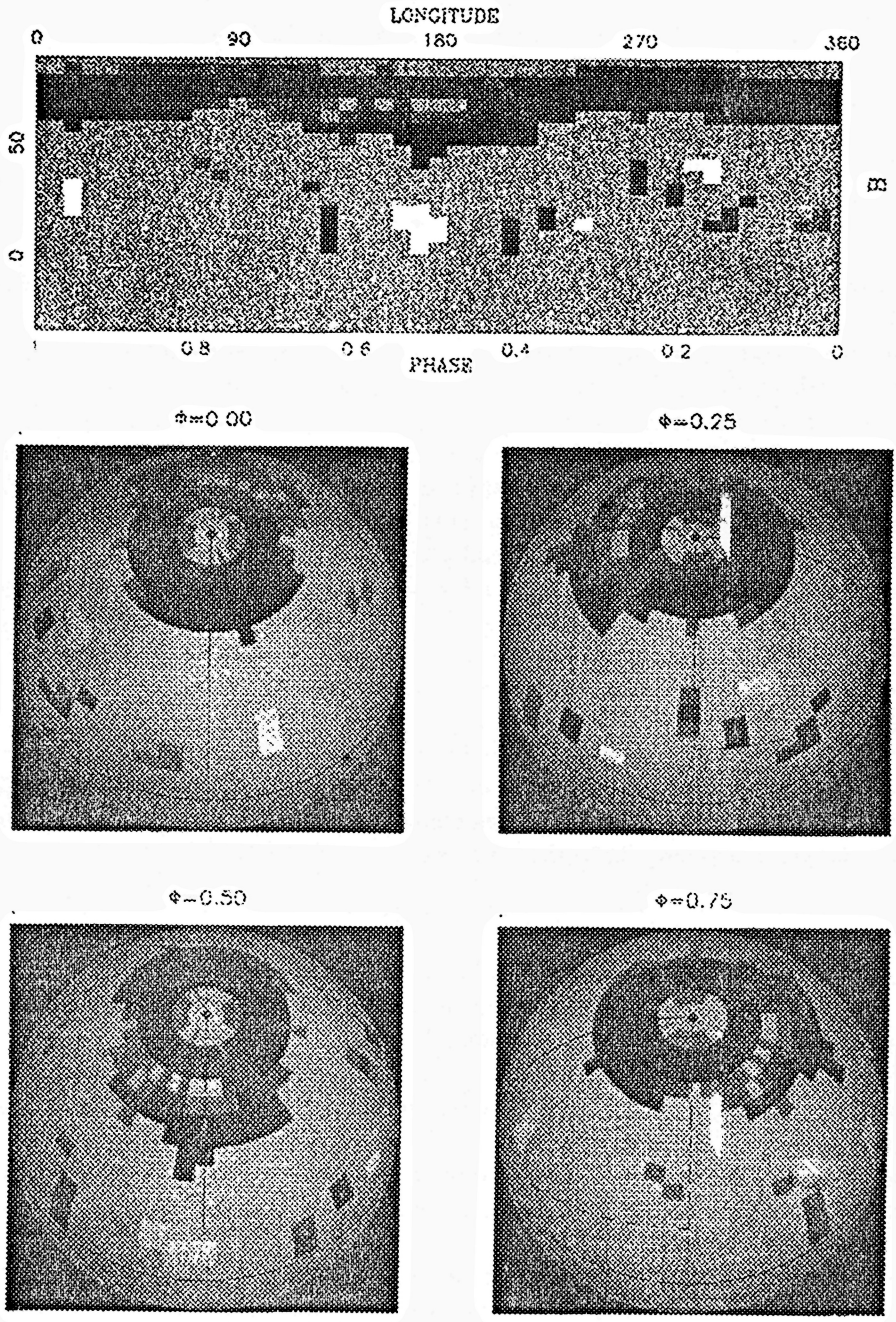

Fig. 6. Unconstrained tomographic image reconstruction of HR 1099 from MUSICOS 1989 (December) data. Darker gray scales depict lower specific intensities.

TABLE I
Stellar parameters used in reconstruction

Parameter	Primary	Secondary
$V_{eq} \sin i (km\,s^{-1})$	38	12
limb darkening ϵ	0.65	0.55
$T_{effective}$ (K)	4500	5730

To calculate the projection matrix, the stellar surface was divided in 45 longitude and 24 latitude bands, defining 980 spatial resolution pixels in the stellar image.

The search strategy employed for the image reconstruction consisted in minimizing χ^2 until reaching the hypersurface χ^2_0 by the constrained gradient method. The entropy was further maximized on the hypersurface $\chi^2 = \chi^2_0$ until reaching the parallelity of the gradients of χ^2 and entropy i.e., practically, until reaching the neighbourhood of the maximum entropy point defined so that cosine of the angle between the gradients is greater or equal to 0.99. The reconstructed image as well as the stellar disc as it would be seen in four successive rotational phases are presented on Fig. 6.

Note that small value of χ^2_0, adopted for this reconstruction, provides the high-frequency details at low latitudes that are likely to be artifacts. While, at this stage, it is not possible to argue if the low-latitude details (bellow 40° are artifacts or not, the high-latitude details are reliable. Particuraly interesting is the dark spot at $\Phi = 0.55$ $B = 50°$ that can be related to the rapid change of the light curve that started to develop at $\Phi \approx 0.55$ during the campaign and evolved, in the next year, towards $\Phi \approx 0.45$ (see Fig. 5). Since, in December 1992, we probably localized the region where the spot was generated, the image reconstruction from the data in 1993 will give the answer concerning its further evolution.

5. DISCUSSION

The photometric and spectroscopic Tomographic Imaging is a powerful tool to spatially resolve the surface and environment of stars providing an access to the information about quasistationnary phenomena. The image resolution and confidence in the reconstructed map are closely related to the global parameters of the star, such as brightness, equatorial velocity, inclination etc. and to the instrumental characteristics as signal-noise ratio, speed or resolution.

These methods have a wide range of application in astrophysics, particularly providing a knowledge of crucial importance to understand the stellar magnetic activity and physical processes related to it.

The objectives of such studies are to obtain the spatial distribution of activity phenomena, to understand the differences with their solar equivalent, to model the active atmospheric regions, to study the correlation between the structures observed at different heights, and monitor the changes associated with active region behaviour, cyclic activity, dynamo phenomena and differential rotation.

The study of solar-type phenomena on spatially resolved stars allows now, for the first time, to intercompare directly activity phenomena on stars and on the sun,

and to understand better solar processes by modelling them on stars with different parameters. On solar-type stars, spots, plages, intense chromospheric/coronal heating, winds, flares and other aspects of stellar activity are fundamentally magnetic in character. The interest for studying chromospheres/coronae of solar-type stars, apart from its own, arise also from the fact that they are excellent laboratories for using, testing and improving radiative transfer and modelling theories under conditions of non-LTE and non radiative equilibrium. It is also possible to diagnose, from the chromospheric/coronal structure and dynamics, the trace of subjacent phenomena associated with the existence of the magnetic fields in stellar surfaces, that are governed by the convective and internal properties of the stars. Some stellar situations allow to isolate better the physical processes at work in the various aspects of stellar activity. The activity relations with stellar parameters give also a tool for studying the global origin and consequences of magnetic field in solar-like stars.

References

Baudrand, J., Böhm, T. : 1992, *Astron. Astrophys.* **259**, 711.

Byrne, P. B. et al. : 1987, *Astron. Astrophys.* **180**, 172.

Catala, C., Foing, B. H., Baudrand, J. et al. : 1993, *Astron. Astrophys.* **275**, 245.

Catalano, S., Rodonò, M. : 1967, *Mem. Soc. Astron. Ital.* **38**, 395.

Deutsch, A. J. : 1970, *Astrophys. J.* **159**, 985.

Falk, A. E., Wehlau, W. H. : 1974, *Astrophys. J.* **192**, 409.

Fekel, F. C., 1983, *Astrophys. J.* **268**, 274.

Goncharskij, A. V., Stepanov, V. V., Khokhlova, V. L., Yagola, A. G. : 1982, *Sov. Astr.* **26**, 690.

Gondoin, P. : 1986, *Astron. Astrophys.* **160**, 73.

Horne, K. D., 1986, *PASP*, **98**, 609.

Jankov, S. : 1987, DEA, Université Paris VII, Meudon Observatory.

Jankov, S., Foing, B. H. : 1987, in *Cool Stars, Stellar Systems, and the Sun*, eds. J. L. Linsky and R. E. Stencel, Springer-Verlag, Berlin Heidelberg, p. 528.

Jankov, S. : 1992, Ph.D. Thesis, Université Paris VII.

Jankov, S., Foing, B. H. : 1992, *Astron. Astrophys.*, **256**, 533.

Jankov, S., Donati, J.-F. : 1994, in Proceedings of the Second MUSICOS workshop, in press.

Khokhlova, V. L., Ryabchikova, T. A. : 1970, *Astrofizika*, **6**, 227.

Khokhlova, V. L., Ryabchikova, T. A. : 1975, *Astr. and Space Science*, **34**, 403.

Mangeney, A., Praderie, F. : 1984, *Astron. Astrophys.* **130**, 143.

Neff, J. : 1988, Ph.D. thesis, University of Colorado, Boulder.

Noyes, R. W., Hartman, C. W., Baliunas, S. L., Duncan, D. K., Vaughan, A. H. : 1984, *Astrophys. J.* **279**, 763.

Ramsey, L. W., Nations, H. L. : 1980, *Astroph. J. Letters*, **348**, L121.

Rodonò, M., Cutispoto, G., Pazzani, V., Catalano, S., Byrne, P. B., Doyle, J. G., Butler, C. J., Andrews, A. D., Blanco, C., Marilli, E., Linsky, J. L., Scaltriti, F., Busso, M., Cellino, A., Hopkins, J. L., Okazaki, A., Hayashi, S. S., Zeilik, M., Helston, R., Henson, G., Smith, P., Simon, T. : 1986, *Astron. Astrophys.* **165**, 135.

Rodonò, M., Byrne, P. B., Neff, J. E., Linsky, J. L., Simon, T., Butler, C. J., Catalano, S., Cutispoto, G., Doyle, J. G., Andrews, A. D., Gibson, D. M. : 1987, *Astron. Astrophys.* **176**, 267.

Semel, M. : 1989, *Astron. Astrophys.* **225**, 456.

Skilling, J., Bryan, R. K. : 1984, *Mon. Not. R. astr. Soc.* **211**, 111.

Titterington, D. M. : 1985, *Astron.Astrophys.* **144**, 381.

Vaughan A. H., Baliunas, S. L., Middelkoop, F., Hartmann, L. W., Mihalas, D., Noyes, R. W., Preston, G. W. : 1981, *Astrophys.J.* **250**, 276.

Vogt, S. S., Penrod, G. D. : 1983, *Publ. Astron. Soc. Pac.* **95**, 565.
Vogt, S. S., Penrod, G. D., Hatzes, A. P. : 1987, *Astrophys. J.* **321**, 496.
Walter, H. M, Neff, J. E., Gibson, D. M., Linsky, J. L., Rodonò, M., Gary, D. E. and Butler C. J : 1987, *Astron. Astrophys.* **186**, 241.